

Designing Topological Bands in Reciprocal Space

N. R. Cooper¹ and R. Moessner²

¹*Cavendish Laboratory, University of Cambridge, J. J. Thomson Ave., Cambridge CB3 0HE, U.K.*

²*Max-Planck-Institut für Physik komplexer Systeme, Nöthnitzer Straße 38, Dresden, Germany*

(Dated: August 23, 2012)

Motivated by new capabilities to realise artificial gauge fields in ultracold atomic systems, and by their potential to access correlated topological phases in lattice systems, we present a new strategy for designing topologically non-trivial band structures. Our approach is simple and direct: it amounts to considering tight-binding models *directly in reciprocal space*. These models naturally cause atoms to experience highly uniform magnetic flux density and lead to topological bands with very narrow dispersion, without fine-tuning of parameters. Further, our construction immediately yields instances of optical Chern lattices, as well as band structures of higher Chern number, $|C| > 1$.

The ability to create new environments for custom-tailored degrees of freedom is central to advancing our understanding of correlated electron physics. In the same way that modulation-doped semiconductor heterostructures gave rise to the field of fractional quantum Hall physics, the creation of artificial gauge fields[1] holds the promise of providing an entirely new perspective on strong-correlation physics in topological bands. The question that naturally arises now is not only how to generate such artificial gauge fields, but also what settings will be most promising for realising new physical phenomena. There is intense current interest in the properties of such systems in condensed matter physics, most recently through the proposed existence of fractional Chern insulators[2–5]. These are lattice systems in which fractional quantum Hall physics occurs in partially filled non-dispersive topological “Chern” bands[6, 7]. These works are all based on tight-binding models, in which band topology and dispersion are controlled by the tunneling matrix elements. The first steps have been taken in implementing tight-binding models of this type for atoms in optical lattices[8], with tunable tunneling phases[9] at least for nearest-neighbour sites[10–12].

Recently it has been demonstrated that topological bands can be formed for ultracold atoms in another, very direct, way[13–15]. Coherent Raman coupling of several ($N > 1$) internal atomic states[1], as used to generate artificial gauge fields[16], allows new forms of optical lattice. In particular, in “optical flux lattices” atoms experience non-zero average magnetic flux density, resulting in low-energy topological bands that are analogous to Landau levels[13, 15]. These new forms of optical lattice are readily implemented in experiment, so it is highly desirable to be able to design their properties. However, they can operate far from the tight-binding limit, so the existing solid-state models cannot be directly applied.

Here, we present a number of insights into the nature of optical flux lattices and develop theoretical tools that allow a targeted design of topological bands in optical lattices. Notably, we show that optical flux lattices are usefully viewed as tight-binding models *in reciprocal space*. This allows a design of band structures by transposing

established results on Chern bands in real space into our new setting. We use our insights to construct three new forms of optical lattice. First, we show how to generate optical flux lattices, involving more than $N = 2$ internal states, for which the magnetic flux density is highly uniform in space. The resulting energy bands have very narrow bandwidth, and recover continuum Landau levels for large N . Second, we show how to construct “optical Chern lattices”, in which the dressed states experience zero net magnetic flux, but for which the band has non-zero Chern number. Finally, we show how one can design optical lattices in which the lowest energy band has Chern number larger than one.

Our results follow from examining the limits of deep/shallow lattices, when the lattice depth \mathcal{V} is large/small compared to the typical kinetic energy $E_R \equiv \hbar^2 \kappa^2 / (2M)$ (all symbols are defined below). After setting up the problem, we discuss these two limits in turn. We comment on possible implementations on the way.

The Hamiltonian for an optically dressed atom with N internal states is[1]

$$\hat{H} = \frac{\mathbf{p}^2}{2M} \hat{\mathbf{1}}_N + \hat{V}(\mathbf{r}) \quad (1)$$

where $\hat{\mathbf{1}}_N$ is the $N \times N$ identity matrix, and $\hat{V}(\mathbf{r})$ an $N \times N$ matrix describing the coherent optical coupling in the rotating wave approximation. The nature of the internal states is unimportant for our purposes: these can be electronic excited states, hyperfine states, or states of orbital motion.

In all cases, the coupling $\hat{V}(\mathbf{r})$ involves absorption/emission of photons from laser beams, so it naturally appears as couplings $V_{\mathbf{k}'-\mathbf{k}}^{\alpha'\alpha} \equiv \langle \alpha', \mathbf{k}' | \hat{V} | \alpha, \mathbf{k} \rangle$, where $|\alpha, \mathbf{k}\rangle$ is the momentum \mathbf{k} eigenstate for component α . We focus on periodic lattices, such that the set of momentum transfers $\{\boldsymbol{\kappa}\}$ for which $V_{\boldsymbol{\kappa}}^{\alpha'\alpha}$ is non-zero forms a regular lattice. The momentum \mathbf{k} of any given component α is then only conserved up to the addition of reciprocal lattice vectors, the basis vectors of which we denote \mathbf{G}_i , with $i = 1 \dots d$ where d is the dimensionality of the lattice. (We focus on lattices in $d = 2$, but the

results can be extended to $d = 3$, with Berry curvature and magnetic flux density becoming pseudovectors.)

By Bloch's theorem, the energy eigenstates of (1) can be assigned crystal momentum \mathbf{q} and band index n , and be decomposed as $|\psi^{n\mathbf{q}}\rangle = \sum_{\alpha, \mathbf{G}} c_{\alpha\mathbf{G}}^{n\mathbf{q}} |\alpha, \mathbf{q} - \mathbf{g}_\alpha - \mathbf{G}\rangle$ where α runs over all N internal states, \mathbf{G} runs over all sites of the reciprocal lattice, and the vectors \mathbf{g}_α account for possible momentum offsets involved in the inter-state transitions. The energy eigenvalues $E_{n\mathbf{q}}$ follow from

$$E_{n\mathbf{q}} c_{\alpha\mathbf{G}}^{n\mathbf{q}} = \epsilon_{\mathbf{q}-\mathbf{g}_\alpha-\mathbf{G}} c_{\alpha\mathbf{G}}^{n\mathbf{q}} + \sum_{\alpha', \mathbf{G}'} V_{\mathbf{g}_\alpha+\mathbf{G}-\mathbf{g}_{\alpha'}-\mathbf{G}'}^{\alpha'\alpha} c_{\alpha'\mathbf{G}'}^{n\mathbf{q}} \quad (2)$$

where $\epsilon_{\mathbf{k}} \equiv \hbar^2 |\mathbf{k}|^2 / (2M)$.

Deep lattice/adiabatic limit: In the limit $E_R/\mathcal{V} \rightarrow 0$ the kinetic energy can be neglected. The effects of the optical coupling in Eqn. (1) can then be fully understood in terms of the local dressed states, the eigenstates of $\hat{V}(\mathbf{r})$. Under adiabatic motion, the n^{th} dressed state experiences magnetic flux density [1] $n_\phi(\mathbf{r}) = \frac{\hat{z}}{2\pi i} \sum_{\alpha} \nabla u_{\alpha}^{n*} \times \nabla u_{\alpha}^n$, due to the Berry curvature [17] associated with spatial variations of its wavefunction $u_{\alpha}^n(\mathbf{r})$. In an optical flux lattice, the lowest energy dressed state experiences $N_\phi \neq 0$ magnetic flux quanta through each unit cell [13].

It is instructive to examine this limit $E_R/\mathcal{V} \rightarrow 0$ also from the point of view of Eqn. (2). Dropping the kinetic energy causes this eigenvalue problem to reduce to that of a *uniform tight-binding model in reciprocal space*, defined by the couplings $V_{\mathbf{g}_\alpha+\mathbf{G}-\mathbf{g}_{\alpha'}-\mathbf{G}'}^{\alpha'\alpha}$ between sites at positions $\mathbf{g}_\alpha + \mathbf{G}$. The energy spectrum of this reciprocal-space tight-binding model – its “bandstructure” – consists of N bands, since there are N sites \mathbf{g}_α associated with each reciprocal lattice point \mathbf{G} . The eigenstates are extended Bloch waves in reciprocal space, and can be written $c_{\alpha\mathbf{G}}^{n\mathbf{r}} \propto e^{i(\mathbf{G}+\mathbf{g}_\alpha)\cdot\mathbf{r}} u_{\alpha}^n(\mathbf{r})$. (For $E_R/\mathcal{V} \rightarrow 0$ the energy is independent of \mathbf{q} and the states are naturally labelled by the band index $n = 1 \dots N$ and a conserved “momentum” \mathbf{r} .)

Crucially, we identify this conserved “momentum” of the reciprocal-space tight-binding model with the real space position \mathbf{r} (and thus its “Brillouin zone” with the real space unit cell). The state in the n^{th} band simply corresponds to the n^{th} local dressed state of $\hat{V}(\mathbf{r})$. The power of this viewpoint emerges upon considering the magnetic flux density n_ϕ : the Berry curvature associated with the adiabatic motion of any dressed state in

real space equals the Berry curvature of the associated band of the reciprocal-space tight-binding model. In particular, the number N_ϕ of magnetic flux quanta through the real space unit cell equals the Chern number of that band. Hence, *the criterion for an optical flux lattice is that the lowest energy band of the reciprocal-space tight-binding model has non-zero Chern number*. Since much is known about the Chern bands of various tight-binding models, this criterion can be used to design optical flux lattices with specific properties.

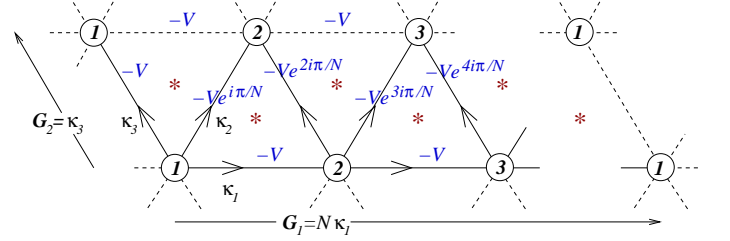


FIG. 1: One primitive unit cell of the reciprocal-space tight-binding model corresponding to the triangular lattice optical flux lattice with N internal states (3), showing the optical couplings $-\mathcal{V}e^{i\phi}$. The clockwise sum of the phases ϕ around any one of the triangular plaquettes is π/N modulo 2π .

One highly desirable feature is to generate a magnetic flux density that is uniform. The resulting energy bands will then closely reproduce Landau levels: topological bands with exact degeneracy, highly susceptible to strong-correlation physics. For all previously proposed optical flux lattices [11, 13, 15] the magnetic flux density is very non-uniform, vanishing at a set of points. This non-uniformity is a mathematical necessity for $N = 2$ [13] and for general N when \hat{V} consists of the generators of $SU(2)$, as in Ref. 15. The above considerations show how to overcome this limitation: one should form a reciprocal-space tight-binding model for which the lowest energy band has uniform Berry curvature.

An optical flux lattice that achieves this goal is illustrated in Fig. 1. The N internal states are arranged on the sites of a triangular lattice, marked by the state label α . The links between lattice sites indicate optical couplings, the displacement in reciprocal space the momentum transfer, with the label marking amplitude and phase. Explicitly, Fig. 1 encodes the coupling matrix

$$\hat{V}(\mathbf{r}) = -\mathcal{V} \begin{pmatrix} 2 \cos(\mathbf{r} \cdot \boldsymbol{\kappa}_3) & A_1 + A_2 e^{-i\frac{\pi}{N}} & 0 & \dots & A_1^* + A_2^* e^{i\frac{\pi(2N-1)}{N}} \\ A_1^* + A_2^* e^{i\frac{\pi}{N}} & 2 \cos(\mathbf{r} \cdot \boldsymbol{\kappa}_3 - \frac{2\pi}{N}) & A_1 + A_2 e^{-i\frac{3\pi}{N}} & \dots & 0 \\ 0 & A_1^* + A_2^* e^{i\frac{3\pi}{N}} & 2 \cos(\mathbf{r} \cdot \boldsymbol{\kappa}_3 - \frac{4\pi}{N}) & \dots & 0 \\ \vdots & \vdots & \vdots & \ddots & \vdots \\ A_1 + A_2 e^{-i\frac{\pi(2N-1)}{N}} & 0 & 0 & \dots & 2 \cos(\mathbf{r} \cdot \boldsymbol{\kappa}_3 - \frac{2\pi(N-1)}{N}) \end{pmatrix} \quad (3)$$

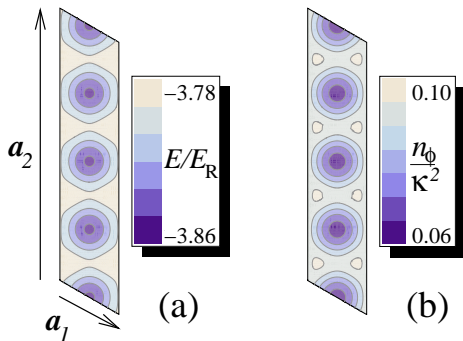


FIG. 2: Spatial dependence of (a) the energy and (b) the magnetic flux density of the lowest energy dressed state of the triangular optical flux lattice (3) for $N = 4$, within a unit cell containing $N_\phi = 1$ flux quantum. Both are highly uniform, becoming increasingly so as $N \rightarrow \infty$.

where $A_j \equiv \exp(-i\mathbf{r} \cdot \boldsymbol{\kappa}_j)$, $\boldsymbol{\kappa}_1 = (1, 0)\kappa$, $\boldsymbol{\kappa}_2 = (\frac{1}{2}, \frac{\sqrt{3}}{2})\kappa$ and $\boldsymbol{\kappa}_3 = \boldsymbol{\kappa}_1 - \boldsymbol{\kappa}_2$. We choose the primitive unit cell of the reciprocal lattice to have basis vectors $\mathbf{G}_1 = N\boldsymbol{\kappa}_1$ and $\mathbf{G}_2 = \boldsymbol{\kappa}_3$; the real-space unit cell then has lattice vectors $\mathbf{a}_1 = \frac{4\pi}{\sqrt{3}\kappa N}(\sqrt{3}/2, 1/2)$ and $\mathbf{a}_2 = \frac{4\pi}{\sqrt{3}\kappa}(0, 1)$.

The properties of the resulting dressed states follow from the bandstructure of the reciprocal-space tight-binding model. The phases on the nearest-neighbour couplings mimic the effect of a uniform magnetic field in reciprocal space (the total phase acquired on hopping around any triangular plaquette being π/N , modulo 2π), so the spectrum follows from Harper's equation for the triangular lattice[18]. For $N \geq 2$ the lowest energy band has Chern number $\mathcal{C} = 1$, implying an optical flux lattice with $N_\phi = 1$ flux quantum per unit cell, *i.e.* mean flux density

$$\bar{n}_\phi = \frac{N_\phi}{|\mathbf{a}_1 \times \mathbf{a}_2|} = \frac{N\sqrt{3}\kappa^2}{8\pi^2}. \quad (4)$$

The local magnetic flux density and the dressed state energy follow from the Berry curvature and dispersion of the lowest energy band of the reciprocal-space tight-binding model. Both show spatial modulations, illustrated in Fig. 2 for $N = 4$. (The spatial dependence of the dressed state takes a form akin to a triangular multi-component Skyrmion lattice[19] with lattice constant $|\mathbf{a}_1|$.) However, as $N \rightarrow \infty$, the reciprocal-space tight-binding model recovers the continuum limit, and its lowest band becomes a degenerate lowest Landau level with uniform Berry curvature. The convergence to uniformity with increasing N is very fast, with corrections that fall exponentially quickly[18, 19].

The emergence, for large N , of highly uniform magnetic flux density distinguishes this optical flux lattice from all previous proposals. Owing to this uniformity, the resulting bandstructure for non-zero kinetic energy, $E_R \ll \mathcal{V}$, closely reproduces the spectrum of a charged

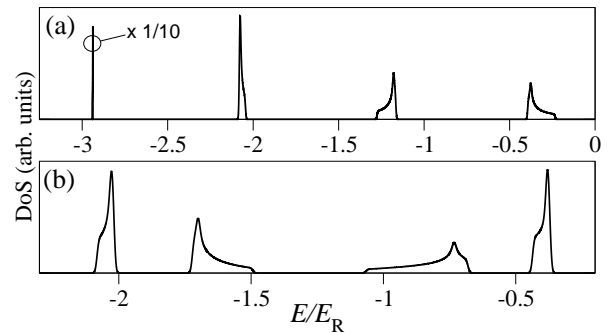


FIG. 3: Low energy density of states for: (a) The triangular optical flux lattice (3) with $N = 4$ internal states and $\mathcal{V} = E_R$; the spectrum closely reproduces the Landau level spectrum, all bands shown having Chern number $\mathcal{C} = 1$. (b) A related model (still with $N = 4$ and $\mathcal{V} = E_R$) in which the phases on the optical couplings are modified as described in the text to form a lowest energy band with Chern number $\mathcal{C} = 2$.

particle in a uniform magnetic field: degenerate Landau levels, spaced by the cyclotron energy $\hbar\omega_c = \frac{\bar{n}_\phi \hbar}{M} = \frac{N\sqrt{3}}{2\pi}E_R$. The fast convergence means that this qualitative structure is already apparent for small N . This is clearly seen in Fig. 3(a) for $N = 4$, for which the lowest energy band has a bandwidth that is about 200 times smaller than the gap to the next band. (For $N = 3$ the same ratio is about 40.)

One can envisage a variety of experimental implementations for lattices of this type, or the many variants that achieve the same end. The case $N = 2$ is the triangular optical flux lattice described in Ref. 13. For $N = 3$ one can use the three components of the $F = 1$ hyperfine manifold of ^{87}Rb [20]. A simple variant is obtained by omitting the state-dependent coupling along $\boldsymbol{\kappa}_3$ (the geometry can then be made square by rotating $\boldsymbol{\kappa}_2 \rightarrow (0, 1)\kappa$). This lattice requires only cyclic coupling over the $N \rightarrow N \pm 1$ states. An implementation of couplings of this kind has been proposed[21] for $N = 4$ using hyperfine levels of ^{87}Rb .

Weak-lattice limit: Further useful results can be obtained by considering the eigenvalue problem (2) in the “nearly-free-electron” limit $\mathcal{V} \ll E_R$. Here, the only influence of the couplings $V_{\boldsymbol{\kappa}}^{\alpha' \alpha}$ is at values of crystal momentum \mathbf{q} close to the lines where two free-particle states are degenerate, where they open up band-gaps. Close to those points \mathbf{q}^* where two (or more) lines cross, the bands can also acquire non-zero Berry curvature. Therefore, one can determine the Chern numbers of the bands in the weak-lattice limit by computing the Berry curvature in the vicinity of these high symmetry points \mathbf{q}^* .

To illustrate the construction, consider the triangular optical flux lattice, Fig. 1, in this limit. The high symmetry points, \mathbf{q}^* , are located at the centres of the triangular plaquettes, at which the kinetic energies of three states (labelled a, b, c) are equal. (These points are

marked by *’s in Fig. 1.) This degeneracy is split by the optical couplings around this plaquette, which we denote $V_{ab} = -\mathcal{V}e^{i\phi_{ab}}$, $V_{bc} = -\mathcal{V}e^{i\phi_{bc}}$, $V_{ca} = -\mathcal{V}e^{i\phi_{ca}}$. Integrating the Berry curvature for the lowest energy state over the vicinity of \mathbf{q}^* shows that the total contribution is $\phi_{\text{tot}} = \text{mod}(\pi + \phi_{ab} + \phi_{bc} + \phi_{ca}, 2\pi) - \pi$. (For $|\phi_{\text{tot}}| = \pi$ the lowest two bands cross at a Dirac point, so the Berry curvature of the lowest energy band is not defined.) For the triangular lattice model (3) the phases are such that $\phi_{\text{tot}} = \pi/N$ for each of the $2N$ plaquettes. Thus we immediately establish that the Chern number of the lowest energy band is $\frac{1}{2\pi} \times (2N) \times (\pi/N) = 1$.

Our approach allows us to design other forms of optical lattice, with topological bands that are not directly related to Landau levels. First we show that one can form optical lattices which have bands with non-zero Chern number, but for which the adiabatic dressed state in real space feels vanishing net flux. In the solid state literature, these are referred to as Chern bands. All previous examples involve tight-binding models in real space, following the seminal work of Haldane[7]. The analogous “optical Chern lattices” that we describe here have the new feature that the magnetic flux density is defined as a *continuous* function of real-space position. A simple example of such an optical Chern lattice is obtained by choosing the triangular optical flux lattice, Eqn. (3), with $N = 2$ and introducing a state-dependent potential $\delta\mathcal{V}\hat{\sigma}_z$. For $\delta\mathcal{V} > 2\mathcal{V}$ the lowest energy dressed state has $\langle\hat{\sigma}_z\rangle < 0$. Hence, the Bloch vector[13] cannot wrap the sphere – the net flux through any unit cell must vanish. However, this additional term does not affect the Berry curvatures at the (four) symmetry points in the Brillouin zone in the weak-lattice limit: the Chern number of the lowest energy band remains $\mathcal{C} = 1$.

Finally, we show how to design an optical lattice for which the lowest energy band has Chern number of magnitude larger than one, $|\mathcal{C}| > 1$, in the weak-lattice limit. One should arrange that the integrated Berry curvatures from all symmetry points \mathbf{q}^* sum to the appropriate value $2\pi\mathcal{C}$. As a concrete example, we adapt the triangular lattice (3) to form a lowest energy band with arbitrary \mathcal{C} by replacing the phases $\frac{\pi}{N}$ appearing in (3), in both diagonal and off-diagonal entries, by $\mathcal{C}\frac{\pi}{N}$. The requirement that the integrated Berry curvature per plaquette lies in the range $-\pi < \mathcal{C}\frac{\pi}{N} < \pi$, leads to $|\mathcal{C}| < N$. Hence, a lowest energy band with $\mathcal{C} = 2$ can be achieved for $N \geq 3$ internal states. Numerical studies for $N = 3, 4$ confirm that the lowest energy band retains $\mathcal{C} = 2$ for $\mathcal{V} \sim E_R$, and even into the deep-lattice limit. The low energy bandstructure for $N = 4$ for $\mathcal{V} = E_R$ is shown in Fig. 3(b). The lowest energy band has Chern number $\mathcal{C} = 2$. The band is well separated from higher bands, the gap to the next band being about 4.5 times its bandwidth, despite the fact that no optimization has been applied.

The methods we have described open the door for the construction of many other forms of optical flux lattice.

Any tight-binding model for which the lowest energy band has non-zero Chern number can be used as the basis for an optical flux lattice. Hence uniform magnetic flux density in real space could also be achieved for a system with fixed N by introducing further-neighbour couplings on the reciprocal-space lattice[22]. Such couplings are readily implemented as higher momentum transfers; indeed, the optical flux lattice proposed in Ref. 15 involves all the couplings of the Haldane model[7]. We have also provided a direct method by which to construct optical lattices with low energy Chern bands of any topology in the weak-lattice limit. This ability to design topological bandstructures, with narrow bandwidth, will allow the use of atomic gases to explore novel correlated topological phases of bosons or fermions in lattice systems.

NRC is grateful to Jean Dalibard for numerous helpful discussions, and RM to Benoît Douçot and Dima Kovrizhin for collaboration on Ref. [19]. This work was supported by EPSRC Grant EP/F032773/1. We thank the Galileo Galilei Institute for hospitality.

-
- [1] J. Dalibard, F. Gerbier, G. Juzeliūnas, and P. Öhberg, *Rev. Mod. Phys.* **83**, 1523 (2011).
 - [2] R. Roy and S. L. Sondhi, *Physics* **4**, 46 (2011).
 - [3] E. Tang, J.-W. Mei, and X.-G. Wen, *Phys. Rev. Lett.* **106**, 236802 (2011).
 - [4] K. Sun, Z. Gu, H. Katsura, and S. Das Sarma, *Phys. Rev. Lett.* **106**, 236803 (2011).
 - [5] T. Neupert, L. Santos, C. Chamon, and C. Mudry, *Phys. Rev. Lett.* **106**, 236804 (2011).
 - [6] D. J. Thouless, M. Kohmoto, M. P. Nightingale, and M. den Nijs, *Phys. Rev. Lett.* **49**, 405 (1982).
 - [7] F. D. M. Haldane, *Phys. Rev. Lett.* **61**, 2015 (1988).
 - [8] M. Lewenstein *et al.*, *Advances in Physics* **56**, 243 (2007).
 - [9] D. Jaksch and P. Zoller, *New Journal of Physics* **5**, 56 (2003).
 - [10] M. Aidelsburger *et al.*, *Phys. Rev. Lett.* **107**, 255301 (2011).
 - [11] K. Jiménez-García *et al.*, *Phys. Rev. Lett.* **108**, 225303 (2012).
 - [12] J. Struck *et al.*, *Phys. Rev. Lett.* **108**, 225304 (2012).
 - [13] N. R. Cooper, *Phys. Rev. Lett.* **106**, 175301 (2011).
 - [14] B. Béri and N. R. Cooper, *Phys. Rev. Lett.* **107**, 145301 (2011).
 - [15] N. R. Cooper and J. Dalibard, *Europhysics Letters* **95**, 66004 (2011).
 - [16] Y.-J. Lin *et al.*, *Nature* **462**, 628 (2009).
 - [17] D. Xiao, M.-C. Chang, and Q. Niu, *Rev. Mod. Phys.* **82**, 1959 (2010).
 - [18] F. H. Claro and G. H. Wannier, *Phys. Rev. B* **19**, 6068 (1979).
 - [19] D. L. Kovrizhin, B. Douçot, and R. Moessner, arXiv:1207.4021.
 - [20] J. Dalibard, private communication.
 - [21] D. L. Campbell, G. Juzeliūnas, and I. B. Spielman, *Phys. Rev. A* **84**, 025602 (2011).
 - [22] E. Kapit and E. Mueller, *Phys. Rev. Lett.* **105**, 215303 (2010).